Clays and Clay Minerals, Vol. 49, No. 4, 347–354, 2001.

HYDROXYL-STRETCHING BANDS IN CURVE-FITTED MICRO-RAMAN, PHOTOACOUSTIC AND TRANSMISSION INFRARED SPECTRA OF DICKITE FROM ST. CLAIRE, PENNSYLVANIA

S. SHOVAL,[1] S. YARIV,[2] K.H. MICHAELIAN,[3] M. BOUDEULLE[4] AND G. PANCZER[4]

[1]Geology Group, Department of Natural Sciences, The Open University of Israel, 16 Klausner St., 61392 Tel Aviv, Israel
[2]Department of Inorganic and Analytical Chemistry, The Hebrew University of Jerusalem, 91904 Jerusalem, Israel
[3]Natural Resources Canada, CANMET Western Research Centre, Devon, Alberta, Canada T9G 1A8
[4]LPCML, UMR 5620 CNRS, Claude Bernard University-Lyon 1, 43 Bd. 11 November 1918, 69622 Villeurbanne Cedex, France

Abstract—The OH-stretching region in curve-fitted micro-Raman, photoacoustic and transmission IR spectra of St. Claire dickite was investigated. Polarized Raman spectra recorded from the (001) and (010) faces of the dickite crystal displayed six prominent OH bands. The relative intensities depend strongly on both the orientation of the crystallographic axes and the direction of the electric vector of the laser beam. Four out-of-plane vibrations, A_A, A_Z, C_A and C_Z, at ~3710, 3706, 3654 and 3643 cm^{-1} respectively, predominate when the electric vector is perpendicular to the dickite plates. Two in-plane vibrations, D_Z and D_A at 3627 and 3623 cm^{-1}, intensify when the electric vector is parallel to the plane. The relationship between band intensity and crystal orientation was interpreted in terms of longitudinal optic (LO) and transverse optic (TO) crystal vibration modes. These LO and TO crystal modes were also observed in curve-fitted photoacoustic and transmission IR spectra of coarse, non-oriented crystals of the dickite.

Key Words—Curve-fitting, Dickite, Infrared, LO and TO Crystal Modes, Micro-Raman, OH bands, SEM.

INTRODUCTION

The OH-stretching region in transmission infrared (IR) spectra of dickites was investigated by Farmer & Russell (1964), Farmer (1974), Prost *et al.* (1989) and Johnston *et al.* (1990). Three prominent OH-stretching bands at 3703, 3655 and 3622 cm^{-1} were observed in these spectra. Following the convention established by Miller & Oulton (1970), Yariv (1986) labeled these bands A, C and D, respectively. Other authors refer to these vibrations as ν_1, ν_3 and ν_4, while Bish and Johnston (1993) assign these bands to OH3, OH2 & OH4 and OH1 vibrations, respectively.

The corresponding region in Raman spectra of dickites was investigated by Wiewiora *et al.* (1979), Pajcini and Dhamelincourt (1994), Frost *et al.* (1996, 1998) and Frost and van der Gaast (1997). Frost *et al.* (1996) studied the Raman spectra of oriented dickite crystals. Altogether these authors observed six different OH bands, and reported different spectra as measured from various faces of the crystal. However, the direction of the electric vector of the incident laser was not reported in their paper.

Recently, Johnston *et al.* (1998) studied the Raman spectra of a single crystal of St. Claire dickite. The authors observed six different polarized Raman spectra from the (001), (010) and (100) faces of large dickite crystals. They showed that band C (in the labeling system of Yariv, 1986) is located at 3643 cm^{-1} in the Raman spectra and at 3655 cm^{-1} in the IR, and concluded that these bands are obtained by combining the stretching vibrations of two different inner-surface OH groups (denoted OH2 & OH4) to form symmetric and asymmetric ν(OH) components. The symmetric vibration is observed mainly in the Raman spectrum at 3643 cm^{-1}, and the corresponding asymmetric ν(OH) component is observed predominantly in the IR at 3655 cm^{-1}. Similarly, Frost *et al.* (1996) identified two bands in the vicinity of band A, at 3711 and 3701 cm^{-1}, in the Raman spectrum of San Juanito dickite.

In 1997, we showed that curve-fitted micro-Raman spectra of dickites exhibit six prominent OH-stretching bands and attributed them to three pairs: bands at ~3710 and 3700 cm^{-1} correspond to the high frequency ν_1 vibration, those at ~3648 and 3635 cm^{-1} arise from the ν_3 vibration, and those at ~3630 and 3623 cm^{-1} are due to the low frequency vibration ν_4 (Shoval *et al.*, 1997). More recently, three pairs of OH-stretching bands were similarly found at 3709 and 3701 cm^{-1}, 3653 and 3646 cm^{-1}, and 3628 and 3623 cm^{-1} in curve-fitted micro-Raman and IR spectra of nacrite (Shoval *et al.*, 2001).

In coarse crystals of kaolinite, Raman spectra exhibit five OH-stretching bands (Wiewiora *et al.*, 1979; Johnston *et al.*, 1985; Michaelian, 1986; Shoval *et al.*, 1995; Frost *et al.*, 1996; Frost and van der Gaast, 1997; Johansson *et al.*, 1998). In previous publications we showed that the high-frequency OH-stretching band of kaolinite consists of a pair of partly overlapping components at ~3697 and 3686 cm^{-1}, which are labeled A and Z, respectively (Shoval *et al.*, 1999a,

1999b). Band Z (Michaelian *et al.*, 1991) was also detected in photoacoustic (Michaelian, 1990; Shoval *et al.*, 1999b) and transmission (Shoval *et al.*, 1999a) IR spectra of kaolinites with a high Hinckley index. The other three features in this region are designated B, C and D, respectively.

The most satisfactory explanation for the appearance of the pair of OH-stretching bands A and Z in spectra of kaolinite consisting of large particles was put forth recently by Farmer (1998, 2000). Macroscopic crystals larger than the wavelength of the exciting radiation possess two long-wavelength crystal vibrations, termed longitudinal optic (LO) and transverse optic (TO) modes; both are associated with the same unit-cell vibration in which the dipole moment is generated. The LO modes have higher frequencies than the corresponding TO modes. In IR spectroscopy, the incident radiation has a much longer wavelength than in Raman spectroscopy. Moreover, transmission IR spectra are traditionally obtained from KBr disks, after grinding the sample/KBr mixture. These factors make observation of both modes difficult in conventional IR spectroscopy, but easier in Raman spectroscopy where sample preparation is usually minimal.

In Raman spectra of kaolinite, the appearance of the bands at ~3697 and 3686 cm^{-1} (bands A and Z) was attributed by Farmer (1998, 2000) to the fact that the wavelength of the laser radiation is short relative to the size of the kaolinite layer. In thin platy kaolinite crystals, where the thickness of the coherent layers is greater than the wavelength of the propagating beam, both LO and TO modes of crystal vibrations may be active in the spectra. Indeed, Shoval *et al.* (1999a, b) recently demonstrated that the 3686 cm^{-1} band (TO frequency) is stronger than the 3697 cm^{-1} band (LO frequency) in Raman spectra of highly-crystallized kaolinites with large coherent domains. On the other hand, when the thickness of the coherent layers is less than the wavelength of the impinging radiation, vibrations perpendicular to the plates produce bands at LO frequencies (bands A, B and C), while those parallel to the larger plates exhibit TO frequencies (band D).

In this paper we describe the observation of three pairs of OH-stretching bands in micro-Raman, photoacoustic and transmission IR spectra of St. Claire dickite. Adapting the model of Farmer (2000) with regard to LO and TO modes in layered clays, it was expected that both modes would occur in spectra of dickite samples for which the thickness of the coherent layers is greater than the wavelength of the impinging beam. To test this model, the sizes of the hexagonal plates and the thickness of the St. Claire dickite crystals were studied by means of SEM micrographs. The relatively large crystal size of this dickite permits measurements of single-crystal micro-Raman spectra, with the incident laser directed along particular crystallographic axes. The differences in the intensities of the OH-stretching bands in the polarized micro-Raman spectra were used to confirm previous reports about the directions of the OH-stretching vibrations in the dickite crystal. The curve-fitted polarized Raman spectra of single-crystal dickite were compared with photoacoustic and transmission IR spectra of coarse, non-oriented dickite crystals and of powdered dickite, respectively.

EXPERIMENTAL METHODS

Dickite from St. Claire, Pennsylvania was purchased from Ward's Natural Science Establishment Inc., Rochester, New York. To measure the micro-Raman and photoacoustic IR spectra, the dickite crystals were used as obtained, without grinding or further purification. The dickite crystals were only ground slightly during the preparation of the KBr disk for transmission IR spectroscopy.

Scanning electron micrographs were obtained using a JEOL (JSM-840) instrument. The dickite crystals were coated with gold.

Micro-Raman spectra were recorded using a Dilor XY confocal micro-Raman spectrometer with a focal length of 500 mm. This instrument is equipped with an Olympus optical microscope, a triple monochromator and a Charge Coupled Device (CCD) EG&G multichannel detector. Spectra were obtained using a 50× objective at a resolution of 3 cm^{-1}. Accumulation times of 360 s were used. The 514.5 nm line of a Spectra Physics 2016 Argon ion laser at a power of 250 mW was used for excitation. Frequencies were calibrated with external and internal standards (521 cm^{-1} Raman band of silicon and argon plasma lines, respectively) and were assumed to have an accuracy of ± 2 cm^{-1} or better. The 2 μm laser spot facilitated measurement of single-crystal micro-Raman spectra. The polarization of the incident and scattered light was parallel (VV = vertical-vertical).

Photoacoustic IR spectra were obtained for unground samples at a resolution of either 4 or 6 cm^{-1} using a Bruker IFS 113v spectrometer and a Princeton 6003 photoacoustic cell. Spectra were recorded at two different mirror velocities to ensure that no artifacts were included.

Transmission IR spectra were recorded using a Nicolet FT-IR spectrometer and "Omnic" software. Disks containing 1 mg of sample in 150 mg of KBr were employed.

Curve-fitting

The micro-Raman and IR spectra were analyzed with the Peak fitting function in "Grams" (Galactic) software. Lorentzian shapes were used for the OH-stretching bands, primarily because these were found to be satisfactory in previous studies of IR spectra of kaolinites and kaolinite complexes (Michaelian *et al.*, 1991). Multiple points on either side of the region of interest were used for baseline linearization. Frequen-

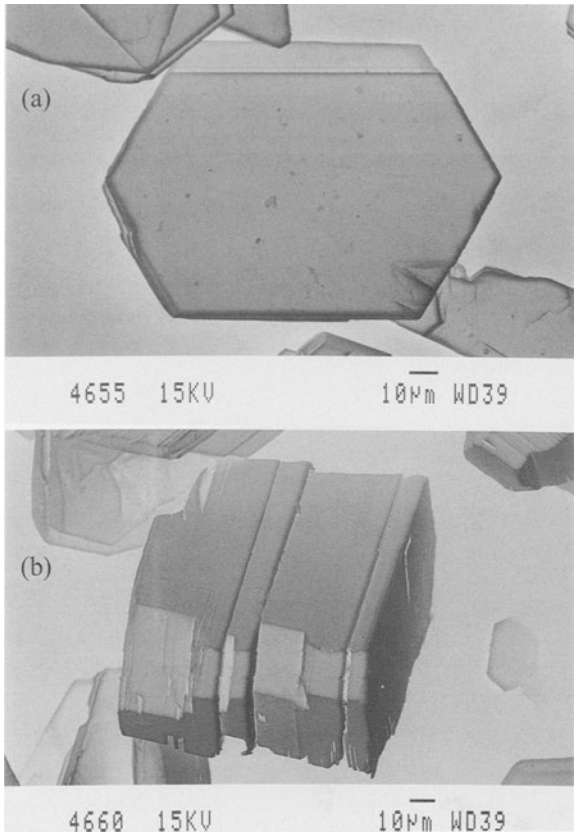

Figure 1. SEM micrographs (negatives) of representative dickite crystals: (a) view along the c' crystallographic axis, illustrating elongated hexagonal plates. Axis a is parallel to the longer (010) face of the crystal, whereas axis b is perpendicular. (b) View along b or a axes displaying a book-type structure, in which coherent layers are separated by cleavage.

cies, widths and band areas were calculated using this software.

Orientation

The directions of the a and b axes in the crystal were determined according to the elongation habit of the plates in the sample examined. Micro-Raman spectra were obtained with the laser along the crystallographic b and c' axes, but not along the a axis. In the last case, the edge between the two faces (110) and $(\bar{1}\bar{1}0)$ of the dickite crystal must be placed on the microscope table, which was impossible in our system. To describe the scattering geometry for different orientations of the crystallographic axes, we used the Porto notation (Swanson, 1973) as adapted for the Raman spectrum of a dickite single-crystal by Johnston *et al.* (1998). As suggested by them, the term c' axis is used since the corresponding spectra were collected at 90° from the (001) face, whereas the c axis makes an angle of 96.5° with respect to this face.

Raman spectra along the c′ axis

In this experiment, the (001) face with the hexagonal plates was placed parallel to the XY plane of the microscope stage and the spectra collected with the laser beam along the c' axis (perpendicular to the (001) face). The $c'(aa)\bar{c}'$ spectrum was collected with the electric vector of the laser beam along the a axis. The $c'(bb)\bar{c}'$ spectrum was recorded after rotating the microscope table through 90° with the electric vector along b.

Raman spectra along the b axis

In this experiment, the (010) face with the cleavage traces was placed parallel to the XY plane of the microscope stage and the spectra collected with the laser beam along the b axis (perpendicular to the (010) face). The $b(c'c')\bar{b}'$ spectrum was collected with the electric vector of the laser beam along c'. The $b(aa)\bar{b}$ spectrum was recorded with the electric vector along the a axis.

Raman spectra along steeply tilted axes

Some spectra were recorded from plates that were inclined with respect to the XY plane of the microscope stage. In this experiment, spectra were obtained with the laser beam impinging between axes a and c' or between axes b and c'. Consequently, the electric vector of the impinging beam was tilted with respect to the axes.

RESULTS

Size of the dickite crystals

Scanning electron micrographs of representative dickite crystals are shown in Figure 1. Elongated hexagonal plates are observed when viewing along the c' axis (Figure 1a). The elongated crystals enable the identification of axes a and b. Axis a is parallel to the longer (010) face of the crystal, whereas axis b is perpendicular. The sizes of the hexagonal plates reach 130 μm along the a axis and 80 μm along the b axis. A book-type structure, in which coherent layers are separated by cleavage planes, is observed in the views along the a or b axes (Figure 1b). The thickness of the crystals in the direction of the c axis is ~100 μm. The thickness of the coherent layers between the cleavage trace reaches 40 μm. In some crystals, the layers are not well bound to each other.

Micro-Raman spectra

The OH-stretching region in the curve-fitted polarized micro-Raman spectra of St. Claire dickite recorded with different crystal orientations is shown in Figures 2–3. Micro-Raman spectra of single-crystal dickite were obtained with the laser beam directed along the b or c' axes. The scaling for each spectrum plotted in the figures is relative to the strongest band in that

https://doi.org/10.1346/CCMN.2001.0490408 Published online by Cambridge University Press

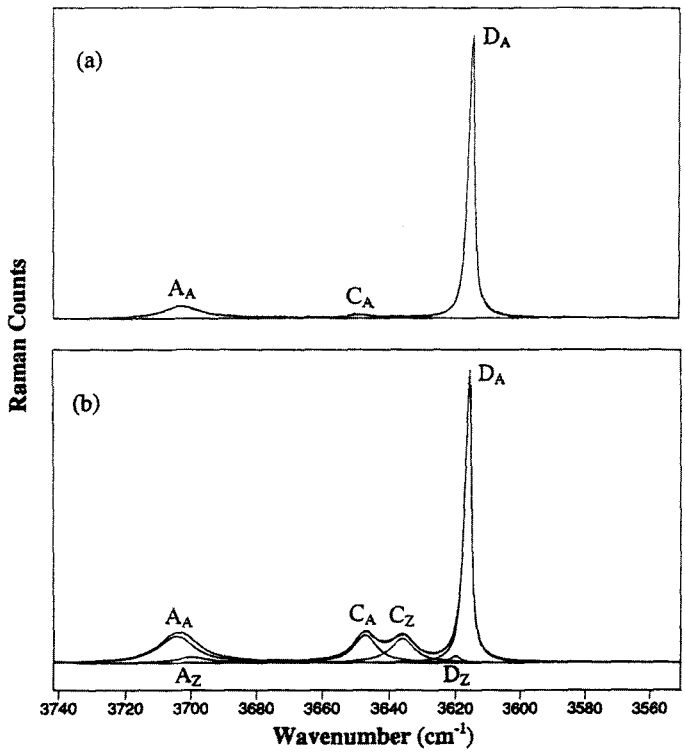

Figure 2. Curve-fitted polarized micro-Raman spectra of single-crystal dickite in the OH-stretching region, collected with the laser beam propagating along the crystallographic c' axis (perpendicular to the (001) face): (a) $c'(aa)\bar{c}'$ spectrum, electric vector along the a axis. The thickness of the coherent layers is less than the wavelength of the impinging beam; (b) $c'(bb)\bar{c}'$spectrum, electric vector along the b axis, but the (001) face was slightly tilted to the XY plane of the microscope stage. The thickness of the coherent layers is greater than the wavelength of the impinging beam.

spectrum (autoscale). Summarizing the findings, the curve-fitted Raman spectra display six prominent bands in the OH-stretching region, at ~3710 and 3706 cm^{-1}, 3654 and 3643 cm^{-1}, and 3627 and 3623 cm^{-1} (Table 1). The relative intensities of these bands depend strongly on both the orientation of the crystallographic axes and on the direction of the electric vector of the laser beam (Figures 2–3). These relative intensities, indicated in Table 1 as strong, medium or weak, should only be considered trends. However, since these ratios are confined to a narrow wavenumber range, it is expected that any inaccuracy will be small. Analysis of the local Raman tensor, which was carried out by Johnston *et al.* (1998), was not conducted during this study. The similarity between the trends in this study and in the work of Johnston *et al.* (1998) supports our observations.

In this work, the OH-stretching bands are labeled A, C and D (Yariv, 1986). Bands which are intense when the direction of the beam is normal to the dickite plates (along crystallographic axis c') are labeled with subscript A, whereas those that are strong when the beam is parallel to the plates (along crystallographic axis b) are accompanied by subscript Z.

Raman spectra along the c' axis

In the $c'(aa)\bar{c}'$ and $c'(bb)\bar{c}'$ positions, the spectra are very similar and so only the former spectrum is presented in Figure 2a. Both spectra show a strong and sharp band at 3623 cm^{-1}, which was attributed by Johnston *et al.* (1998) to OH1, and very weak bands at 3654 and 3710 cm^{-1}, attributed by these authors to (OH2 & OH4) and OH3, respectively. These bands are labeled D_A, C_A and A_A, respectively, here. In these spectra, band D_A of the inner hydroxyl groups, which arises from nearly in-plane vibrations, is intense, while bands C_A and A_A of the inner-surface hydroxyl groups, which arise from nearly out-of-plane vibrations, are weak. In these spectra, even after careful curve-fitting, it was impossible to identify the bands D_Z, C_Z and A_Z (observed in the other spectra at 3627, 3643 and 3706 cm^{-1}, respectively). Here, the thickness of the coherent layers in the dickite crystal examined is less than the wavelength of the impinging beam, therefore the weak vibrations perpendicular to the plates only produce bands at LO frequencies (bands A_A and C_A, Figure 2a), while vibrations parallel to the larger plates exhibit a TO frequency (band D_A). These results are

https://doi.org/10.1346/CCMN.2001.0490408 Published online by Cambridge University Press

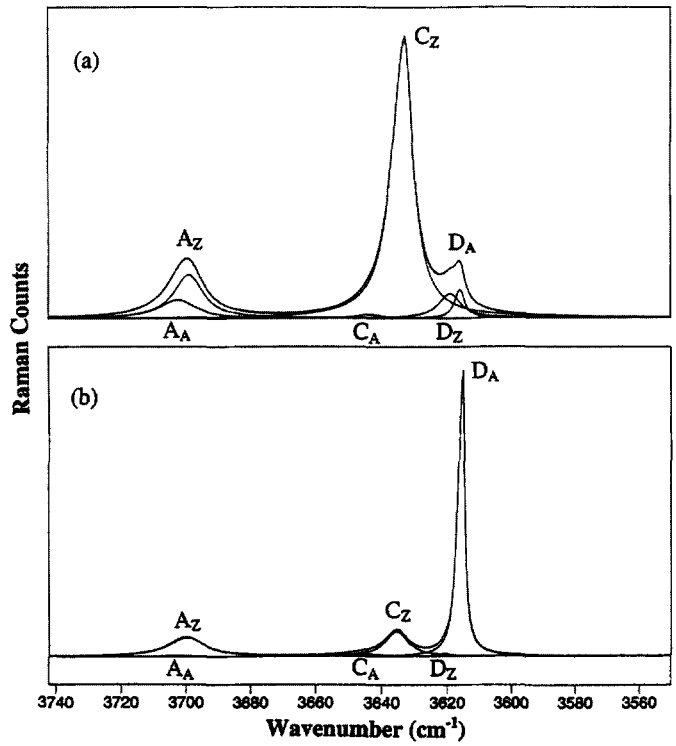

Figure 3. Curve-fitted polarized micro-Raman spectra of single-crystal dickite in the OH-stretching region, collected with the laser beam propagating along the crystallographic *b* axis (perpendicular to the (010) face) with VV polarization: (a) $b(c'c')\bar{b}$ spectrum, electric vector along the c' axis; (b) $b(aa)\bar{b}$ spectrum, electric vector along the *a* axis.

in agreement with Johnston *et al.* (1998) who obtained only a trace of a band at 3643 cm^{-1} in their $c'(aa)\bar{c}'$ spectrum.

Figure 2b depicts a micro-Raman spectrum approximately along the c' axis in the $c'(bb)\bar{c}'$ position, but with the (001) face slightly tilted to the XY plane of the microscope stage. This means that the direction of the laser beam is slightly tilted relative to the c' axis of the sample and the electric vector is oriented mainly along the *b* axis, with a small contribution along *c*. In this case, the apparent thickness of the coherent layers in the dickite crystal examined is greater than the wavelength of the impinging beam and both LO and TO vibrations are observed. Comparison with the spectrum in Figure 2a demonstrates that this spectrum (Figure 2b) also shows a very strong and sharp D_A band, but the stronger bands C_A and A_A are due to the contributions of the electric vectors in the *b* direction. Bands D_Z, C_Z and A_Z are also observed in this spectrum.

Raman spectra along the b axis

In the $b(c'c')\bar{b}$ and $b(aa)\bar{b}$ positions, the spectra are markedly different. In the $b(c'c')\bar{b}$ spectrum the C_Z band of the inner hydroxyls is most intense, and is accompanied by a weak C_A band (Figure 3a). The

Table 1. Crystal vibration modes in curve-fitted micro-Raman, photoacoustic and transmission IR spectra of St. Claire dickite in the OH-stretching region.

Spectra	Crystal vibration modes (cm^{-1})						Chi^2	RMS
	A_A	A_Z	C_A	C_Z	D_Z	D_A		
Raman spectra								
$c'(aa)\bar{c}'$ and $c'(bb)\bar{c}'$	3710W	ND	3654VW	ND	ND	3623VS	0.004	684.3
$b(c'c')\bar{b}$	3710W	3706M	3652VW	3642VS	3627W	3624W	0.060	866.5
$b(aa)\bar{b}$	3710VW	3706W	3652VW	3642W	3627W	3622VS	0.004	249.3
IR spectra								
Photoacoustic	3714M	3705M	3657S	3644W	3627W	3623S	6.5	0.001
Transmission	3712M	3703M	3655M	3644W	3627VW	3622S	4.7	0.004

ND = not detected, W = weak, M = medium, S = strong, V = very.

https://doi.org/10.1346/CCMN.2001.0490408 Published online by Cambridge University Press

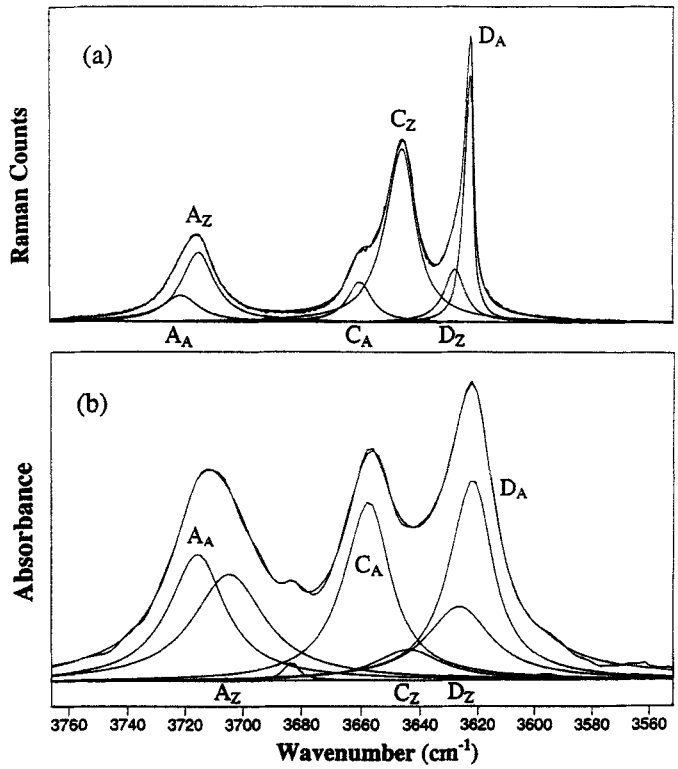

Figure 4. The OH-stretching region in: (a) curve-fitted polarized micro-Raman spectrum of single-crystal dickite, collected with the laser beam propagating along tilted axes; (b) curve-fitted photoacoustic IR spectrum of unground dickite crystals.

inner-surface hydroxyl bands A_A and A_Z are relatively intense, while the inner hydroxyl bands D_Z and D_A are weak. In the $b(aa)\bar{b}$ spectrum the opposite is true, the D_A inner hydroxyl band is most intense and the D_Z band is weak (Figure 3b). The inner-surface hydroxyl bands C_A and C_Z, as well as bands A_A and A_Z, are weak.

Raman spectra along steeply tilted axes

In these spectra both inner OH bands D_Z and D_A, and inner-surface OH bands C_A and C_Z, as well as inner-surface bands A_A and A_Z, are clearly observed (Figure 4a).

Photoacoustic and transmission IR spectra

Curve-fitting results in the OH-stretching region of photoacoustic IR spectra are illustrated in Figure 4b. The photoacoustic IR spectrum of dickite was obtained without grinding. Six prominent OH-stretching bands were observed at 3714 and 3705 cm^{-1}, 3657 and 3644 cm^{-1}, and 3627 and 3623 cm^{-1} in the curve-fitted spectrum (Table 1). In addition to these bands, a weak band was observed at 3684 cm^{-1}.

Six prominent OH-stretching bands were observed at 3712 and 3703 cm^{-1}, 3655 and 3644 cm^{-1}, and 3627 and 3622 cm^{-1} in the curve-fitted transmission IR spectrum of a very lightly ground KBr disk of dickite (Table 1).

DISCUSSION

LO and TO crystal modes of OH-stretching vibrations

Farmer (2000) presented a theoretical discussion on the OH-stretching bands in Raman spectra of thin platy crystals of kaolinite-like minerals. In dickite, the sizes of the hexagonal plates (Figure 1a) are larger than the wavelength of the radiation. According to Farmer's theoretical discussion, a Raman spectrum recorded with the beam along the *b* axis should show LO and TO crystal vibration modes. The occurrence of the band pairs for dickite at ~3710 and 3706 cm^{-1}, 3654 and 3643 cm^{-1}, and 3627 and 3623 cm^{-1} can also be interpreted in terms of LO and TO crystal vibration modes. The three band pairs are labeled A_A and A_Z, C_A and C_Z, and D_Z and D_A, respectively.

A Raman spectrum recorded with the beam along the c' axis is determined by the thickness of the coherent layers (Figure 1b). Where the thickness of the coherent layers is less than the wavelength of the impinging beam, vibrations perpendicular to the plates produce bands at LO frequencies (bands A_A and C_A), while those parallel to the larger plates exhibit TO

https://doi.org/10.1346/CCMN.2001.0490408 Published online by Cambridge University Press

frequencies (band D_A) (Figure 2a). Where the apparent thickness of the coherent layers is greater than the wavelength of the propagating beam, both LO and TO crystal vibration modes may be active in the spectra (Figure 2b). Farmer (2000) attributed the 3655 and 3643 cm^{-1} bands in the Raman spectrum of St. Claire dickite observed by Johnston *et al.* (1998) to the LO and TO crystal modes of the OH2 & OH4 vibrations.

The crystal modes LO and TO were also observed in curve-fitted photoacoustic IR spectra of coarse and non-oriented crystals of St. Claire dickite (Figure 4b), and these are similar to those observed in the Raman spectra. The photoacoustic IR spectrum can be considered as representative of several non-oriented single crystals. In this sense, it can be compared to the single-crystal Raman spectra discussed above. According to the Raman study these bands are labeled A_A, A_Z, B_A, C_A, C_Z, D_Z and D_A (Table 1). However, in contrast to the polarized Raman spectra which depend heavily on the orientation of the crystal, the photoacoustic IR spectrum is not known to vary with orientation.

In-plane and out-of-plane vibrations

Intercalation and deuteration studies have established that the bands at 3703 and 3655 cm^{-1} (bands A and C) in IR spectra of dickite arise from inner-surface hydroxyls, whereas the 3622 cm^{-1} band (band D) is due to inner OH groups (Farmer, 1974). By analogy, the crystal modes A_A, A_Z, C_A and C_Z are attributed to inner-surface OH groups, whereas modes D_A and D_Z are due to inner OH groups. Orientation studies showed that the inner-surface OH bands at 3703 and 3655 cm^{-1} arise from groups nearly perpendicular to the plates (out-of-plane), whereas the 3622 cm^{-1} inner OH band arises from groups nearly parallel to the plates (in-plane) (Farmer, 1974; Brindley *et al.*, 1986; Yariv, 1986). Yariv (1986) studied the deuteration of kaolin group minerals, and obtained a polarized IR spectrum of a deuterated dickite. A careful examination of the IR spectrum (Figure 2 in his study) shows that there is an intensification of band C″ when the angle between the incident IR beam and an oriented film of deuterated dickite increases. This intensification is greater than that displayed by band A″ in the same experiment. In this labeling scheme, the (″) symbol signifies that bands A″ and C″ arise from OD groups obtained by deuterating the OH groups responsible for bands A and C, respectively.

According to Johnston *et al.* (1998), band A at 3707 cm^{-1} in Raman spectra of dickite arises from the vibration of OH3 groups that make an angle of 51.9° with the (001) plane and have an O-H. . .O distance of 314 pm, the longest of the inner-surface OH groups. Band C at 3643 cm^{-1} is due to the vibrations of OH2 & OH4 groups, which occur at angles of 75.5° and 74.1° with the 001 plane and yield O-H. . .O distances of 294 and 296 pm respectively. Band D at 3623 cm^{-1} is due to the vibration of OH1 groups that create an angle of −1.3° with the (001) plane.

The polarized micro-Raman spectra in this study confirm the observations of previous IR (Farmer, 1974) and Raman (Johnston *et al.*, 1998) studies of dickite which indicated that the bands near 3703 and 3655 cm^{-1} (A and C, respectively) arise from almost out-of-plane vibrations, whereas the band at ~3622 cm^{-1} (D) is due to a nearly in-plane vibration. Inner OH bands D_Z and D_A, which arise from nearly in-plane vibrations, are intense in the $c'(aa)\bar{c}'$, $c'(bb)\bar{c}'$ and $b(aa)\bar{b}$ spectra (Figures 2a, 2b and 3b), in which the incident laser is polarized along the crystallographic a or b axes parallel to the dickite plates. The inner-surface OH bands C_A and C_Z, as well as A_A and A_Z, which originate from nearly out-of-plane vibrations, are intensified in the $b(c'c')\bar{b}$ spectrum (Figure 3a) obtained with the incident laser polarized along the c' axis, perpendicular to the dickite plates. When the impinging laser beam is tilted with respect to both axes, the nearly in-plane and out-of-plane vibrations are clearly observed (Figure 4a), due to contributions along axes a and c' or b and c'.

ACKNOWLEDGMENTS

This work was supported by The Open University of Israel Research Fund. This support is gratefully acknowledged.

REFERENCES

Bish, D.L. and Johnston, C.T. (1993) Rietveld refinement and Fourier transform infrared spectroscopic study of the dickite structure at low temperature. *Clays and Clay Minerals,* **41,** 297–304.

Brindley, G.W., Kao, C., Harrison, J.L., Lipsiscas, M. and Raythatha, R. (1986) Relation between the structural disorder and other characteristics of kaolinites and dickites. *Clays and Clay Minerals,* **34,** 233–249.

Farmer, V.C. (1974) The layer silicates. Pp. 331–363 in: *The Infrared Spectra of Minerals* (V.C. Farmer, editor). Monograph **4.** Mineralogical Society, London.

Farmer, V.C. (1998) Differing effects of particle size and shape in the infrared and Raman spectra of kaolinite. *Clay Minerals,* **33,** 601–604.

Farmer, V.C. (2000) Transverse and longitudinal crystal modes associated with OH stretching vibrations in single crystals of kaolinite and dickite. *Spectrochimica Acta Part A,* **56,** 927–930.

Farmer, V.C. and Russell, J.D. (1964) The infrared spectra of layer silicates. *Spectrochimica Acta,* **20,** 1149–1173.

Frost, R.L. and van der Gaast, S.J. (1997) Kaolinite hydroxyls—a Raman microscopy study. *Clay Minerals,* **32,** 471–484.

Frost, R.L., Fredericks, P.M. and Shurvell, H.F. (1996) Raman microscopy of some kaolinite clay minerals. *Canadian Journal of Applied Spectroscopy,* **41,** 10–14.

Frost, R.L., Tran, T.H., Rintopl, L. and Kristof, J. (1998) Raman microscopy of dickite, kaolinite and their intercalates. *Analyst,* **123,** 611–616.

Johansson, U., Frost, R.L., Forsling, W. and Kloprogge, J.T. (1998) Raman spectroscopy of the kaolinite hydroxyls at 77 K. *Applied Spectroscopy,* **52,** 1277–1282.

Johnston, C.T., Sposito, G. and Birge, R.R. (1985) Raman spectroscopic study of kaolinite in aqueous suspension. *Clays and Clay Minerals,* **33,** 483–489.

Johnston, C.T., Agnew, S.F. and Bish, D.L. (1990) Polarized single-crystal Fourier-transform infrared microscopy of Ouray dickite and Keokuk kaolinite. *Clays and Clay Minerals,* **38,** 573–583.

Johnston, C.T., Helsen, J., Schoonheydt, R.A., Bish, D.L. and Agnew, S.F. (1998) Single-crystal Raman spectroscopic study of dickite. *American Mineralogist,* **83,** 75–84.

Michaelian, K.H. (1986) The Raman spectrum of kaolinite #9 at 21°C. *Canadian Journal of Chemistry,* **64,** 285–289.

Michaelian, K.H. (1990) Step-scan photoacoustic infrared spectra of kaolinite. *Infrared Physics,* **30,** 181–186.

Michaelian, K.H., Yariv, S. and Nasser, A. (1991) Study of the interactions between caesium bromide and kaolinite by photoacoustic and diffuse reflectance infrared spectroscopy. *Canadian Journal of Chemistry,* **69,** 749–754.

Miller, J.G. and Oulton, J.D. (1970) Protropy in kaolinite during percussive grinding. *Clays and Clay Minerals,* **18,** 313–323.

Pajcini, V. and Dhamelincourt, P. (1994) Raman study of OH-stretching vibrations in kaolinite at low temperature. *Applied Spectroscopy,* **48,** 638–641.

Prost, R., Damene, A.S., Huard, E., Driard, J. and Leydecker, J.P. (1989) IR study of the structural OH in kaolinite, dickite and nacrite and poorly crystalline kaolinite at 5 to 600 K. *Clays and Clay Minerals,* **37,** 464–468.

Shoval, S., Boudeulle, M., Panczer, G. and Yariv, S. (1995) Raman micro-spectrometry and infrared spectroscopy study of the alteration products of trachyte sills and dykes in Makhtesh Ramon area, Israel. Pp. 325–337 in: *Physics and Chemistry of Dykes* (G. Baer and A. Heimann, editors). Balkema, Rotterdam.

Shoval, S., Michaelian, K.H., Boudeulle, M., Panczer, G. and Yariv, S. (1997) OH stretching Raman active modes in dickite. Pp. 108 in: *Program and Abstracts, Annual Meeting of the Geological Society of Israel,* Kefar Gil'adi, Israel.

Shoval, S., Yariv, S., Michaelian, K.H., Lapides, I., Boudeulle, M. and Panczer, G. (1999a) A fifth OH-stretching band in IR spectra of kaolinites. *Journal of Colloid and Interface Science,* **212,** 523–529.

Shoval, S., Yariv, S., Michaelian, K.H., Boudeulle, M. and Panczer, G. (1999b) Hydroxyl-stretching bands 'A' and 'Z' in Raman and infrared spectra of kaolinites. *Clay Minerals,* **34,** 551–563.

Shoval, S., Yariv, S., Michaelian, K.H., Boudeulle, M. and Panczer, G. (2001) LO and TO crystal modes of the hydroxyl stretching vibrations in micro-Raman and infrared spectra of nacrite. *Optical Materials,* **16,** 311–318.

Swanson, B.I. (1973) General notation for polarized Raman scattering from gases, liquids, and single crystals. *Applied Spectroscopy,* **27,** 382–385.

Wiewiora, A., Wieckowski, T. and Sokolowska, A. (1979) The Raman spectra of kaolinite sub-group minerals and of pyrophyllite. *Archiwum Mineralogiczne,* **135,** 5–14.

Yariv, S. (1986) Interactions of minerals of the kaolin group with cesium chloride and deuteration of the complexes. *International Journal of Tropical Agriculture,* **IV(4),** 310–322.

E-mail of corresponding author: shoval@oumail.openu.ac.il

(*Received 10 November 1999; revised 23 August 2000; Ms 395; A.E. Jessica Elzea Kogel*)